A Molecular-Dynamics Simulation Study of the Conformational Preferences of Oligo(3-hydroxyalkanoic acids) in Chloroform Solution

Peter J. Gee[1]), **Fred A. Hamprecht**, **Lukas D. Schuler**, and **Wilfred F. van Gunsteren***

Laboratorium für Physikalische Chemie, ETH-Hönggerberg, CH-8093 Zürich

and **Elke Duchardt**[2])[3]), and **Harald Schwalbe**[3])

Department of Chemistry, Francis Bitter Magnet Laboratory, Massachusetts Institute of Technology, 170 Albany Street, Cambridge, MA 02139, USA

and **Matthias Albert**[2]) and **Dieter Seebach**

Laboratorium für Organische Chemie, ETH Hönggerberg, CH-8093 Zürich

The GROMOS96 molecular-dynamics (MD) program and force field was used to calculate the conformations at 298 K in $CHCl_3$ solution of two hexakis(3-hydroxyalkanoic acids). One consists of (*R*)-3-hydroxybutanoate (HB) residues only: H–(OCH(Me)–CH_2–CO)$_6$–OH (**1**). The other one carries the side chains of valine, alanine, and leucine: H–(OCH($CHMe_2$)CH_2–CO–O–CH(Me)–CH_2–CO–O–CH(CH_2 $CHMe_2$)–CH_2–CO)$_2$–OH (**2**), with homochiral 3-hydroxyalkanoate (HA) moieties. In both cases, the conformational equilibria were sampled 2500 times for 25 ns. Other than clusters of arrangements with inter-residual hydrogen bonding (between the O- and C-terminal OH and COOH groups, and with chain-bound ester carbonyl O-atoms; *Fig. 6*), there are no preferred backbone conformations in which the molecules **1** and **2** spend more than 5% of the time. Specifically, neither the 2_1- nor the 3_1-helical conformation of the oligoester backbone (found in stretched fibers, in lamellar crystallites, and in single crystals of polymers PHB and of oligomers OHB) is sampled to any significant extent (*Fig. 8* and *9*), in spite of the high population, in both oligomers, of the (–)-*synclinal* conformation around the C(2)–C(3) bond (angle ϕ_2 in *Fig. 2*). In contrast to β-oligopeptides, for which strongly preferred secondary structures are found after a few ns, and for which the number of conformations levels off with time, the number of conformational clusters of the corresponding oligoesters found by our force-field MD calculations increases steadily over the observation time of 25 ns (*Fig. 5*). Thus, the conclusion from biological and physical-chemical studies, according to which the PHB chain is extremely flexible, is confirmed by our computational investigation: in $CHCl_3$ solution, the hexakis(3-hydroxyalkanoate) chain samples its conformational space *randomly*!

1. Introduction. – Associated with the biological role of the short-chain poly[(*R*)-3-hydroxybutanoate] (PHB) [1], which has been shown to allow the passage of ions across phospholipid bilayer membranes under voltage-driven and concentration-driven conditions [2], or to function as a transmembrane ion-channel when associated with Ca polyphosphate [1–3], is the question of its secondary structure. From the investigation of PHB or PHB derivatives in the solid state, two different folding patterns were recognized: a 2_1 helix in stretched fibers [4] and in lamellar crystallites of the polymer

---

[1]) Part of the Master Thesis (Diplomarbeit) of *P. J. G.*, ETH Zürich, 2001.

[2]) Part of the projected Ph. D. Theses of *M. A.* (ETH Zürich) and of *E. D.* (MIT).

[3]) Present Address: Institut für Organische Chemie, Johann Wolfgang Goethe-Universität Frankfurt, Marie-Curie-Strasse 11, D-60439 Frankfurt.

[5], and both, 2_1 and 3_1 helices in crystals of cyclic oligomers (oligolides) of HB [6]. To gain information about the conformation of the PHB backbone in homogeneous, isotropic solution – phospholipid bilayers in which the short chain PHB are incorporated may be considered solutions in a two dimensional nonpolar solvent! – investigations on the structure of PHB in solution were undertaken. Although there are hints for the presence of folded secondary structures on the very short time scale of UV/VIS spectroscopy (provided by FRET (*F*luorescence *R*esonance *E*nergy *T*ransfer) [7] and CD [8][9] measurements), no predominant secondary structure has been discovered on the longer NMR time scale[4]). The conclusion was that PHB possesses a highly flexible backbone. A method to study the conformation of individual members of the PHB population in solution is the application of molecular-dynamics calculations. We present here a simulation of oligo(3-hydroxyalkanoate) (OHA) hexamers **1** and **2** (*Fig. 1*). The validity of computer simulations for the prediction or calculation of secondary structures is well-documented by the work of *Seebach*, *Jaun*, and *Van Gunsteren* on β-peptides: the helical and turn structures of β-peptides were simulated successfully [12], using a force field originally developed for α-peptides, thus demonstrating its applicability for oligomers other than those for which it had been conceived.

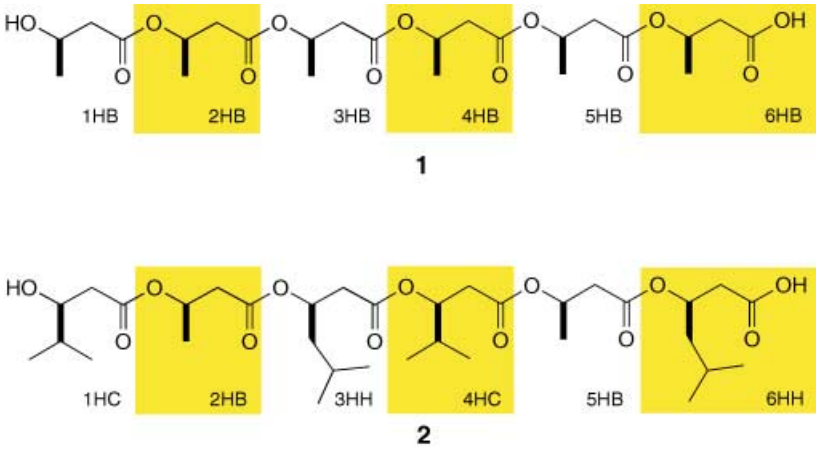

Fig. 1. *Formulae of the molecules* **1** *and* **2**, *and numbering and abbreviations for the residues* (*cf.* [11])

2. Methods. – *Molecular Models.* The labeling conventions and abbreviations that are used throughout this report are shown in *Figs. 1* and *2*. The topology of each molecule was constructed with parameters of the GROMOS96 43A1 force field [14]. This force field, though designed for biomolecules such as peptides and sugars, was calibrated to general thermodynamic properties of the common functional groups of

[4]) 2D-NMR Measurements revealed persistent secondary structures for β-peptides [10], the amide analogs of PHB; because of its long time scale, this technique is appropriate only for molecules that adopt well-populated or long-lived secondary structures; it fails and gives only average values in the case of rapidly interconverting secondary structures. For detailed discussions on investigations of OHA derivatives **1** and **2** by NMR, see our previous papers [7][8] and the accompanying publication [11].

organic chemistry (*e.g.*, example, densities, and heats of vaporization). The parameters used to model the backbones of the molecules **1** and **2** are given in *Tables 1* and *2*. Those for the side chains were the standard GROMOS96 43A1 parameters of the amino acid residues Ala, Leu, and Val [14]. The so-called charge groups required by the force field are indicated in *Fig. 3*. The $CHCl_3$ model was taken from [14][15].

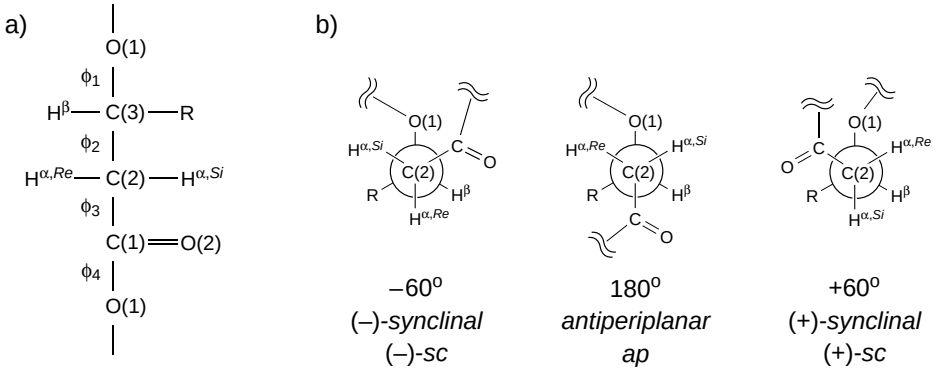

Fig. 2. *Specification of backbone dihedral angles and selected H-atoms in the β-hydroxy ester chains of* **1** *and* **2**. *a*) Backbone dihedrals are defined as: $\phi_1 = (C(1)-O(1)-C(3)-C(2))$; $\phi_2 = (O(1)-C(3)-C(2)-C(1))$; $\phi_3 = (C(3)-C(2)-C(1)-O(1))$; $\phi_4 = (C(2)-C(1)-O(1)-C(3))$. *b*) Designation of dihedral angles ϕ_2 (sign of the angle according to *Prelog-Klyne* descriptors [13]).

Table 1. *Nonbonded Interaction Parameters for the Backbone in* **1** *and* **2**. IAC refers to the integer atom code used to reference *Van der Waals* parameters in the GROMOS96 suite of programs [14]. Atoms C(2) and C(3) are 'united' atoms, representing CH_n groups.

Atom	Description	IAC	Partial charge [e]
H	hydroxylic hydrogen	18	0.398
O(1)	ester O-atom	3	−0.360
C(3)	C(β)	12	0.160
C(2)	C(α)	13	0.000
C(1)	carbonyl C-atom	11	0.580
O(2)	carbonyl O-atom	1	−0.380
O(1)	carboxyl O-atom	3	−0.548
H	carboxyl H-atom	18	0.398

Simulations. The MD simulations of molecules **1** and **2** were performed with the GROMOS96 program [14][16] and the GROMOS96 43A1 force field [14]. They were run with $CHCl_3$ as the solvent in a cubic box at 298 K and at 1 atm pressure, with the temperature and pressure being maintained by weak coupling to an external bath [17]. The coupling time for the thermostat was 0.1 ps. For the barostat, it was 0.5 ps. An isothermal compressibility of $1.6107 \cdot 10^{-3}$ [kJ mol^{-1} nm^{-3}]$^{-1}$ [15] was used. In both cases, periodic boundary conditions were employed, and a triple-range scheme with cut-off radii of 0.8 nm/1.4 nm was used for all nonbonded interactions, the long-range forces being updated after every fifth time step. Outside the longer cut-off radius, a reaction-field approximation [18] was used with a relative dielectric permittivity of 4.8 [15]. The initial conformation of both molecules was an extended conformation (*i.e.*,

Table 2. *Intramolecular Interaction Parameters for the Backbone of the Oligoesters*

Bond-stretching parameters			
Bond	b_0 [nm]	K_b [kJ mol^{-1}nm^{-4}]	
H–O(1) (O-terminus)	0.100	15.7	
O(1)–C(3)	0.143	8.18	
C(3)–C(2)	0.153	7.15	
C(2)–C(1)	0.153	7.15	
C(1)–O(2)	0.123	16.6	
C(1)–O(1) (C-terminus)	0.136	10.2	
Bond-angle bending parameters			
Bond angle	θ_o [degree]	K_θ[kJ mol^{-1}]	
H–O(1)–C(3)	109.5	450	
O(1)–C(3)–C(2)	109.5	520	
O(1)–C(3)–C(4)	109.5	520	
C(2)–C(3)–C(4)	109.5	520	
C(3)–C(2)–C(1)	111.0	530	
C(2)–C(1)–O(2)	121.0	685	
O(2)–C(1)–O(1)	124.0	730	
C(2)–C(1)–O(1)	115.0	610	
C(1)–O(1)–C(3)	109.5	450	
C(1)–O(1)–H	109.5	450	
Improper dihedral-angle parameters			
Dihedral angle	ξ_o [degree]	K_ξ[kJ mol^{-1}degree^{-2}]	
C(3)–C(2)–O(1)–C(4)	35.26439	0.102	
C(1)–C(2)–O(1)–O(2)	0.0	0.051	
Dihedral-angle torsional parameters			
Dihedral angle	cos (δ)	m	K_ϕ [kJ mol^{-1}]
O(1)–C(3)–C(2)–C(1)	+1.0	3	5.860
O(1)–C(3)–C(2)–C(1)	+1.0	2	0.418
C(3)–C(2)–C(1)–O(1)	+1.0	6	1.000
C(2)–C(1)–O(1)–C(3)	−1.0	2	16.700
C(1)–O(1)–C(3)–C(1)	+1.0	3	1.260
C(2)–C(1)–O(1)–H	−1.0	2	16.700

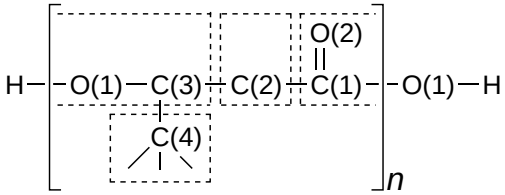

Fig. 3. *Charge groups used in the calculation of nonbonded interactions in molecules* **1** *and* **2**. The atomic charges of a charge group (indicated by dashed lines) add up to zero. When applying a nonbonded interaction cut-off radius, either all or none of the atoms of a charge group are taken into account in the nonbonded pair list or interaction [14].

that with all backbone dihedral angles set to 180°). The timestep used in solving the equations of motion was 0.002 ps. Covalent bonds were kept rigid with a relative precision of 10^{-4} according to the procedure SHAKE [19]. The motion of the center of mass was removed at regular intervals (every 2 ps). *Table 3* summarizes the simulation specifications. Both simulations covered 25 ns.

Table 3. *Specification of Simulation Parameters*

System		
Solute	**1**	**2**
Number of solute atoms	39	49
Number of solvent molecules	657	657
box type	cubic	
initial box length [nm]	4.5	
timestep [ps]	0.002	
center of mass motion removed every [psec]	2	
Nonbonded interactions		
pair-list cut-off radius [nm]	0.8	
nonbonded interaction cut-off radius [nm]	1.4	
pair-list update frequency [ps^{-1}]	100	
Thermodynamic restraints		
temperature coupling at [K]	298.15	
using coupling time of [ps]	0.1	
pressure coupling at [atm]	1	
using coupling time of [ps]	0.5	

Cluster Analysis. The cluster analysis performed was the same for the two molecules, and the method was used as described in the [20]. In each case, structures were extracted from the trajectory at 0.01-ns intervals for analysis (a total of 2500 structures per simulation). The clustering was performed in Cartesian space. For each structure, a least-squares translational and rotational fit was performed with the backbone atoms of residues 2–5 (terminal residues were not taken into account, as they tend to have more freedom of motion), and the atom-positional root-mean-square difference (RMSD) for this set of atoms was calculated. With a RMSD ≤ 0.1 nm for the set of backbone atoms as a criterion of similarity of two structures, the number of neighbors (*i.e.*, structures satisfying the similarity criterion) for each of the structures in the initial pool of 2500 was determined. The structure with the highest number of neighbors was then taken as the central member of the first-ranked cluster. All structures belonging to this cluster were thereafter removed from the pool. For each of the remaining structures, the number of neighbors was again computed. The structure with the most neighbors became the central member of the second cluster of structures. Structures belonging to this second cluster were then also removed from the pool. This process was iterated, until all the structures were assigned to a cluster. This type of clustering favors the most common structures and ensures a minimum difference in atom-positional RMSD between central members of clusters equal to the similarity criterion. It also results in many 'clusters' with only one member. These are not necessarily structures that are very different from structures in other clusters, but they

lie just outside other clusters. In general, they have similar (neighbor) structures (RMSD ≤ 0.1 nm) in other clusters.

Investigating Helix Similarity. The 2_1- and 3_1-model helices were considered, with experimentally determined ideal angles. These are shown in *Table 4*. For each structure in the trajectory, a least-squares fit to each of the helix models was performed on the backbone atoms of residues 2–5. The atom-positional RMSD for this set of atoms was then calculated.

Table 4. *Values of Dihedral Angles, ϕ_i for the Helical Structures of Poly[(*R*)-3-hydroxybutanoate]* [1][4–6]. See *Fig. 2* for designation of angles and other conventions.

Angle type	Value in left-handed 2_1 helix [degrees]	Value in right-handed 3_1 helix [degrees]
ϕ_1	149.9	142.2
ϕ_2	– 56.1	– 62.3
ϕ_3	– 43.3	150.7
ϕ_4	– 174.2	– 176.9

Extraction of Rotamer Populations. The relative population of each rotameric state was extracted from the relevant dihedral time series with angle filters: $120 < \phi_i < 240$ (*ap*); $-120 < \phi_i < 0$ ((−)-*sc*); $0 < \phi_i < 120$ ((+)-*sc*).

Calculation of J-*Coupling Constants.* Scalar coupling constants were calculated for vicinal H,H coupling about the torsional angle ϕ_2 (see *Fig. 2* for labels). Two calculations were performed. One was based on the standard *Karplus* relationship (*Eqn. 1*) [21]:

$$^3J = a_1\cos^2\phi + a_2\cos^2\phi + a_3 \tag{1}$$

The other was based on the generalized *Karplus* relationship (*Eqn.* 2) [22]:

$$^3J = a_1\cos^2\phi + a_2\cos^2\phi + a_3 + \Sigma_i\Delta x_i[a_4 + a_5\cos^2[\xi_i\phi + a_6\,|\,\Delta x_i\,|\,]] \tag{2}$$

The sum is over the substituents of the atoms forming the bond axis of the torsional angle ϕ; Δx_i is the electronegativity difference with respect to the H-atom of the first atom of the substituent; ξ_i is a chirality parameter that determines the relative orientation of the substituent i with respect to the HC–CH fragment.

The parameters used in the calculations are summarized in *Tables 5* and *6*. The parameters for the calculations with the *Karplus* relationship are standard values for vicinal couplings in amino acids[5]) and are, therefore, approximate for ester moieties. The parameters for the generalized *Karplus* relationship were taken from [22]. The atomic electronegativities reported by *Huggins* [24] were used.

3. Results. – *Comparison of Calculated and Experimentally Determined Quantities.* The local and global conformational characteristics of molecule **2** have been investigated by NMR techniques [11]. In particular, the population of rotameric states about dihedral angles ϕ_2 have been deduced from measurements of vicinal J values,

[5]) As given, *e.g.*, in [23].

Table 5. *Parameters of the* Karplus *Relationships* (*Eqns. 1* and *2*) *Used to Calculate* J*-Coupling Constants.* Values are taken from [22][23].

Calculation	a_1	a_2	a_3	a_4	a_5	a_6
H,H coupling (standard *Karplus*)	8.7	−1.6	0.7	–	–	–
H,H coupling (generalized *Karplus*)	13.22	−0.99	0.00	0.87	−2.46	19.9

Table 6. *Atomic Electronegativities* (relative to hydrogen) *and Chirality Parameters* ξ_i *Used with the Generalized* Karplus *Relationship* (*Eqn. 2*). See *Fig. 2* for designation of atoms.

Atom	Relative electronegativity	$\xi_{H^{\alpha,Re}}$	$\xi_{H^{\alpha,Si}}$
O(1)	1.3	1	1
C(4)	0.4	−1	−1
C(1)	0.4	−1	1

according to a three-state model *Pachler* analysis and on the assumption of fast rotameric interconversion. Dihedral angles ϕ_2 were chosen for two reasons: they are the ones most amenable for the application of NMR techniques, and a (−)-*sc* conformation is a characteristic feature of both helices proposed as model structures for PHB[6]).

In *Table 7*, vicinal *J*-coupling constants calculated as time averages over the simulation trajectories are compared with measured values [11]. With the two *Karplus*

Table 7. *Vicinal* ^{3}J*-Coupling Constants* (in Hz) *in molecule* **2**. Trajectory averages calculated with the two different *Karplus* equations and measured values [11].

Residue	Data source	$^3J(H^{\beta},H^{\alpha,Re})$ [Hz]	$^3J(H^{\beta},H^{\alpha,Si})$ [Hz]
1 HC	MD, *Eqn. 1*	2.8	6.4
	MD, *Eqn. 2*	2.9	7.1
	Experiment	2.7	9.7
2 HB	MD, *Eqn. 1*	2.0	9.2
	MD, *Eqn. 2*	0.5	11.1
	Experiment	4.6	7.6
3 HH	MD, *Eqn. 1*	2.3	9.2
	MD, *Eqn. 2*	0.8	11.1
	Experiment	5.3	< 5.3
4 HC	MD, *Eqn. 1*	3.7	6.3
	MD, *Eqn. 2*	3.7	7.2
	Experiment	5.9	4.9
5 HB	MD, *Eqn. 1*	2.2	8.6
	MD, *Eqn. 2*	1.0	10.2
	Experiment	4.9	7.4
6 HH	MD, *Eqn. 1*	2.0	9.6
	MD, *Eqn. 2*	0.3	11.7
	Experiment	–	–

[6]) See our recent papers [7][8], the accompanying publication in this issue [11], a review article [1], and leading references cited therein.

relationships (*Eqns. 1* and *2*), similar values are obtained (average absolute difference is 1.3 Hz), although a variation of up to 2.1 Hz is observed. The difference between simulated and measured values is, on average, 2.2 Hz with *Eqn. 1*, and 3.3 Hz with *Eqn.* 2. These values are by 0.9 to 1.9 Hz larger than the uncertainty in the simulated values due to the use of a particular *Karplus* relationship.

In *Table 8*, the values for the populations of the rotameric states obtained in the experimental study and the values calculated from the MD-simulation trajectory are compared: in both cases, the (−)-*sc* rotamer is highly populated for all residues. This suggests that there is a chance that either of the proposed (left-handed 2_1 and right-handed 3_1)[5]) helical conformations is adopted for some length of time. However, experimental NOE (ROE) data collected for molecule **2** provide no further evidence for significant population of helical structure in the NMR analysis.

Table 8. *Comparison of Simulated* (Sim.) *and Experimentally* (Exper.) *Derived Conformation Populations about Torsional Angles* ϕ_2 *in* **2**. A dash indicates that experimental data are not available. The experimental populations were derived from vicinal *J*-coupling constants and a three-state model [11].

Residue	Population [%] of conformation (ϕ_2)					
	ap (180°)		(−)-*sc* (− 60°)		(+)-*sc* (60°)	
	Sim.	Exper.	Sim.	Exper.	Sim.	Exper.
1 HC	9	5	56	77	35	18
2 HB	5	24	88	55	7	21
3 HH	10	–	89	–	1	–
4 HC	19	34	54	23	27	43
5 HB	4	27	82	53	14	20
6 HH	4	–	92	–	3	–

The observed differences in fine detail (for example, the relative magnitude of the rotameric populations down the molecular chain in each case) are discussed in the following section.

General Conformational Characteristics of Molecules **1** *and* **2**. Cluster analysis of the 25-ns trajectory of molecule **1** shows that the most stable conformation (first-ranked cluster) is adopted less than 5% of the time. The molecule spends *ca.* 10% of its time in the first three clusters. For the rest of the time, it more or less freely samples its conformational space. This is illustrated in *Fig. 4*,*a*, and, from *Fig. 5*, it is evident that the number of clusters has not levelled off after 25 ns of simulation, and that the molecule continues to sample unvisited regions of conformational space.

The prevailing conformations of the hexakis[(*R*)-3-hydroxybutanoic acid] (**1**) are stabilized by inter-residual H-bonds. One of these is shown in *Fig. 6*,*a*, a graphic of the central member conformation of the first-ranked cluster. The percent occurrence of the various H-bonds that form during the simulation are summarized in *Table 9*. The two H-bond donors in the molecule are involved 47 and 26% of the time in different intramolecular H-bonding.

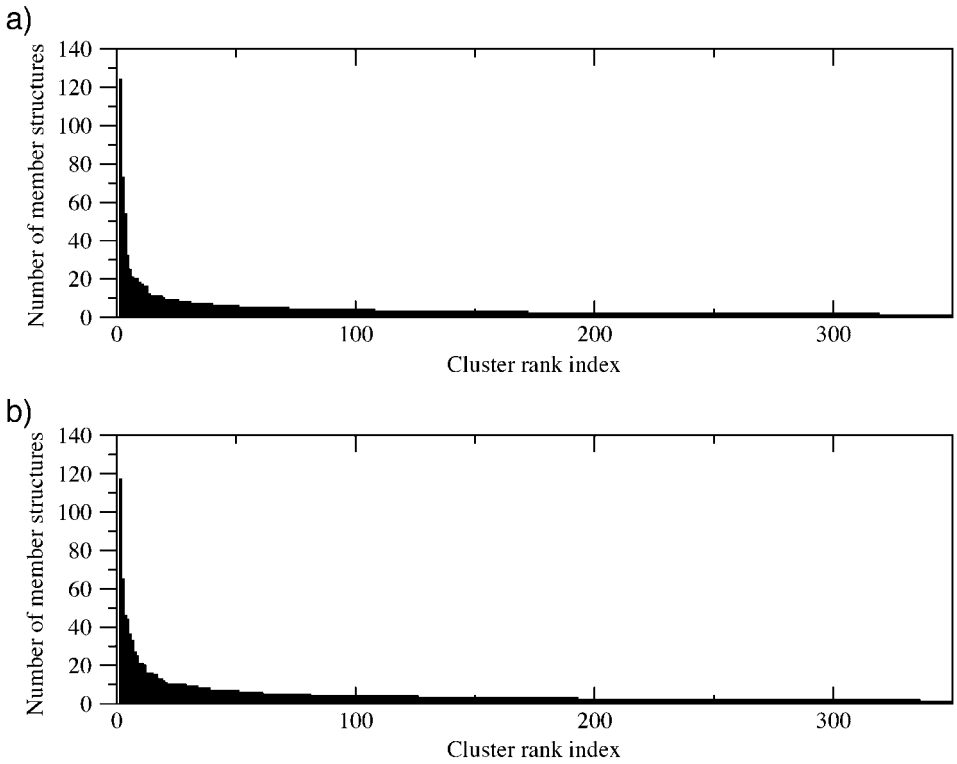

Fig. 4. *Number of structures per cluster as a function of cluster rank number* (starting from the most populated cluster). *a*) Hexa(3-hydroxybutanoic acid) derivative **1**; *b*) Hexa(3-hydroxyalkanoic acid) derivative **2**. Only the most populated clusters are shown. The cluster analysis is based on 2500 MD trajectory structures lying 10 ps apart.

In *Fig. 7,a*, we show *Ramachandran*-type plots of **1** summarizing the torsional angle distributions of the molecule[7]). Angle ϕ_2, for example, generally adopts values of *ca.* 300° (*i.e.*, $-60°$, the (−)-*sc* rotamer). The wide distribution of angle ϕ_1 in 1 HB reflects the fact that the O-terminal OH group of the chain rotates freely at this temperature. For the other residues, it hovers around 110°. The angle ϕ_3 more or less 'avoids' values near the *trans* or *ap* conformation.

The atom-positional RMSD (backbone; residues 2–5) from the left-handed 2_1 helix, suggested as a possible stable structure for PHB in solution[5]), shows that the helix is not sampled to any significant extent (*Fig. 8,a*)[8]); similarity criterion: RMSD

---

[7]) The ester dihedral angle C(2)–C(1)–O(1)–C(3), ϕ_4, has not been included, since it is essentially stiff at 180°. This theoretical and experimental observation is reflected in the large force constant for rotation about this bond (see *Table 2*).

[8]) Please note: the trajectory used to generate *Fig. 8* is not the same as that for which other data is presented, but comes from a related run where a slight bias was given to *sc* rotamers about torsional angles ϕ_2. This does not affect the conclusions drawn from the simulation data. Since the 2_1 model helix requires adoption of a *sc* rotamer for angles of this type, it may be taken as more compelling evidence that this structure is not a stable configuration both for molecule **1** and for molecule **2**.

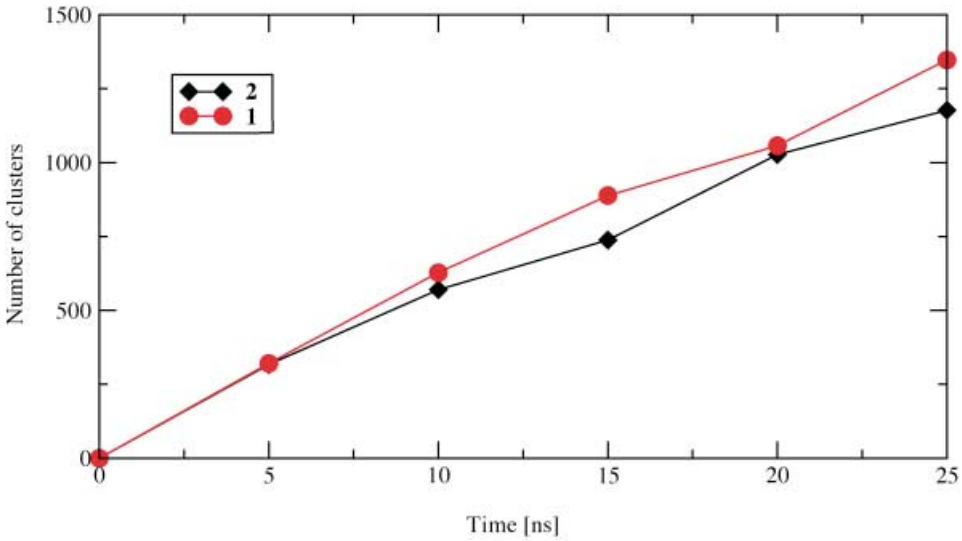

Fig. 5. *Number of conformational clusters formed by molecules* **1** *and* **2** *as a function of time*

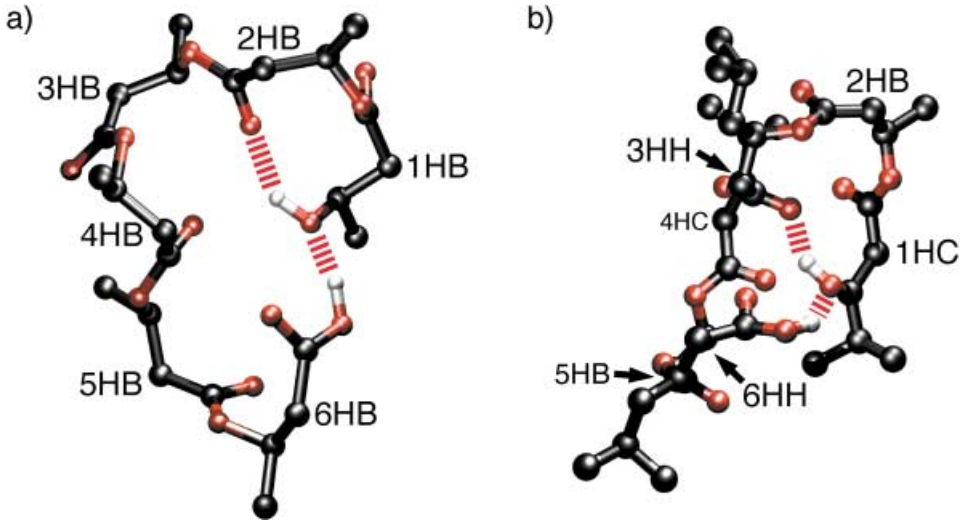

Fig. 6. *H-Bonded structures of* a) **1** *and* b) **2** The models shown are those of the central member structures of the first-ranked clusters.

≤ 0.08 nm). A similar result is found for the right-handed 3_1 helix model[5]) conformation (*Fig. 9,a*).

The overall conformational characteristics of the hexakis(3-hydroxyalkanoic acid) **2** in $CHCl_3$ (again over 25 ns) are similar to those of the HB derivative **1**. Cluster analysis (*Fig. 4,b*) shows that the most stable conformation (first-ranked cluster) is again adopted less than 5% of the time. The molecule spends *ca.* 10% of its time in the three most highly populated conformations. Again, the most stable conformations are

Table 9. *H-Bonding in the 25-ns Simulations of Molecules* **1** *and* **2**. A H-bond is assumed to exist if the H-acceptor distance is smaller than 0.25 nm and the donor–H–acceptor angle is larger than 135°.

Hexakis(3-hydroxybutanoic acid) **1**		
Donor atom	Acceptor atom	Percent occurrence
1 HB, O(1)	1 HB, O(2)	4.9
1 HB, O(1)	2 HB, O(2)	18.8
1 HB, O(1)	2 HB, O(1)	3.3
1 HB, O(1)	3 HB, O(2)	7.8
1 HB, O(1)	3 HB, O(1)	2.2
1 HB, O(1)	4 HB, O(2)	5.9
1 HB, O(1)	6 HB, O(2)	3.8
6 HB, O(1) (Carboxy)	1 HB, O(2)	7.6
6 HB, O(1) (Carboxy)	1 HB, O(2)	6.8
6 HB, O(1) (Carboxy)	2 HB, O(2)	7.8
6 HB, O(1) (Carboxy)	3 HB, O(2)	4.1
Hexakis(3-hydroxyalkanoic acid) **2**		
Donor atom	Acceptor atom	Percent occurrence
1 HC, O(1)	1 HC, O(2)	6.9
1 HC, O(1)	2 HB, O(2)	5.1
1 HC, O(1)	3 HH, O(2)	20.5
1 HC, O(1)	4 HC, O(2)	11.3
1 HC, O(1)	6 HH, O(2)	2.6
6 HH, O(1) (Carboxy)	2 HB, O(2)	14.5
6 HH, O(1) (Carboxy)	3 HH, O(2)	9.0
6 HH, O(1) (Carboxy)	4 HC, O(2)	3.8
6 HH, O(1) (Carboxy)	4 HC, O(1)	2.6

stabilized by H-bonds (*Table 9*). The two H-bond donors in the molecule are 36 and 30% of the time involved in different intramolecular H-bonds. The torsional angle-correlation plots (*Fig. 7,b*) show again, as for **1** but less pronounced, that torsional angle ϕ_2 generally favors a (–)-*sc* rotamer. They also show that the distribution of angle ϕ_3 of residue 4 HC is different from that of the same angle type in other residues. This may be due to steric effects caused by the bulky i-Bu groups of residues 3 HH and 6 HH. As for molecule **1**, the H-bonds are shown in the central structure of the first-ranked cluster of the trajectory of **2** (*Fig. 6,b*).

4. Discussion. – *Conformational Profile of the HB Oligomer* **1** *and the Effect of Side-Chain Modifications in* **2**. The simulation of **1** shows that, to all intents and purposes, the molecule samples its conformational space randomly. No conformations of significant stability are adopted. This is strikingly clear when one considers that the most stable conformation is adopted only 5% of the time. In contrast, a β-heptapeptide (at 298 K; MeOH solution) has been shown [20] to adopt a single conformation 97% of the time[9]). That neither the left-handed 2_1- nor the right-handed 3_1-helical conformation, suggested as structures of PHB[5]), are significantly stable in solution is perhaps not

[9]) Also, a relatively stable helical structure of an 'aminoxy' tripeptide was observed, both experimentally [25] and by simulation [26] in $CHCl_3$.

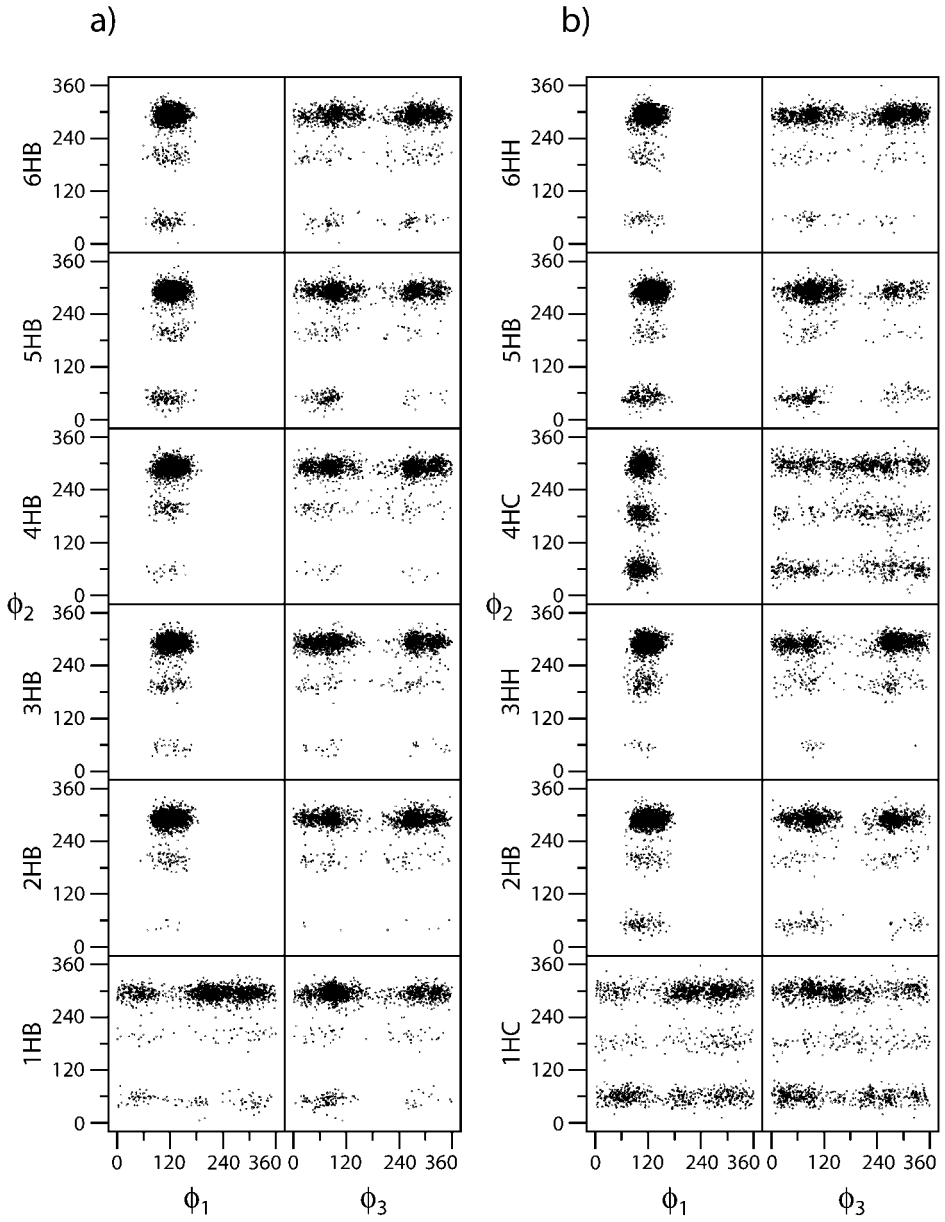

Fig. 7. *Calculated* Ramachandran*-type plot of dihedral angles* ϕ_1, ϕ_2, *and* ϕ_3 *for molecules* **1** (a) *and* **2** (b)

surprising: the most stable conformations adopted by the two molecules under consideration seem to be stabilized by inter-residue H-bonding. Since PHB possesses only H-bond donors at the chain ends, in a longer-chain molecule the effects of intramolecular H-bonding would be expected to be much reduced.

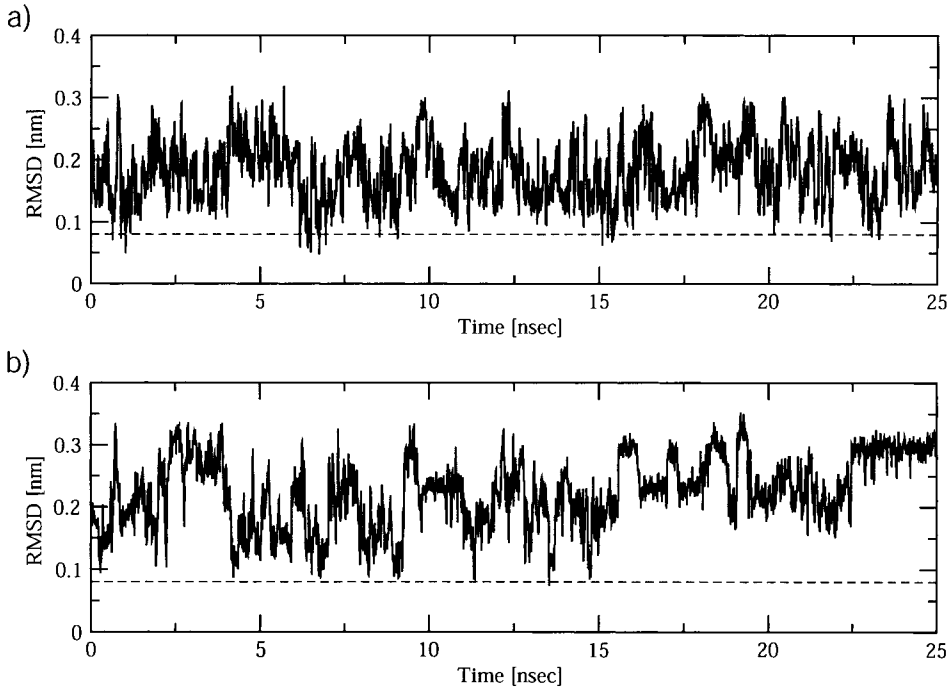

Fig. 8. *Trajectory atom-positional RMSD for molecules* **1** (a) *and* **2** (b) *from the left-handed* 2_1*-helix model*. In both cases, the RMSD was calculated for the configuration defined by the set of backbone atoms of residues 2–5 and the first atom of each side chain of these residues. See *Footnote 8* for details of this calculation.

A comparison of the simulation of the hexamer **2**, which carries different side chains, with that of the 'homo'-oligomer **1**, which consists of HB units only, shows that the addition of branched alkyl substituents has not significantly altered the conformational behavior of the molecule.

Comparison of Simulation Results with Those Derived from NMR Measurements. It has been noted above that the results of the simulation regarding rotameric populations about the key dihedral angle O–CHMe–CH_2–CO (ϕ_2) agree qualitatively with those obtained in an NMR study but for residue 4 HC: the (−)-*sc* conformation is highly populated in all residues. In the fine details, however, differences are apparent. There are only a few values that may be compared, but, with those available (*Table 8*), it seems that the simulation generates populations of *sc* conformation on ϕ_2 higher than those derived from NMR data, and also that, for residue 1 HC (in **2**), it gives a population of the (−)-*sc* conformation that is noticeably lower than that indicated by the NMR data. The apparent bias towards *sc* conformations most probably arises from the fact that the parameters used to describe torsional angles ϕ_2 are not optimal. However, both MD and NMR data reveal that the overall conformation is random.

5. Conclusions. – This report has presented the results of 25-ns simulations of a poly[(*R*)-3-hydroxybutanoate] (PHB) hexamer fragment and a derivative of this fragment with different side chains synthesized for the purposes of an NMR

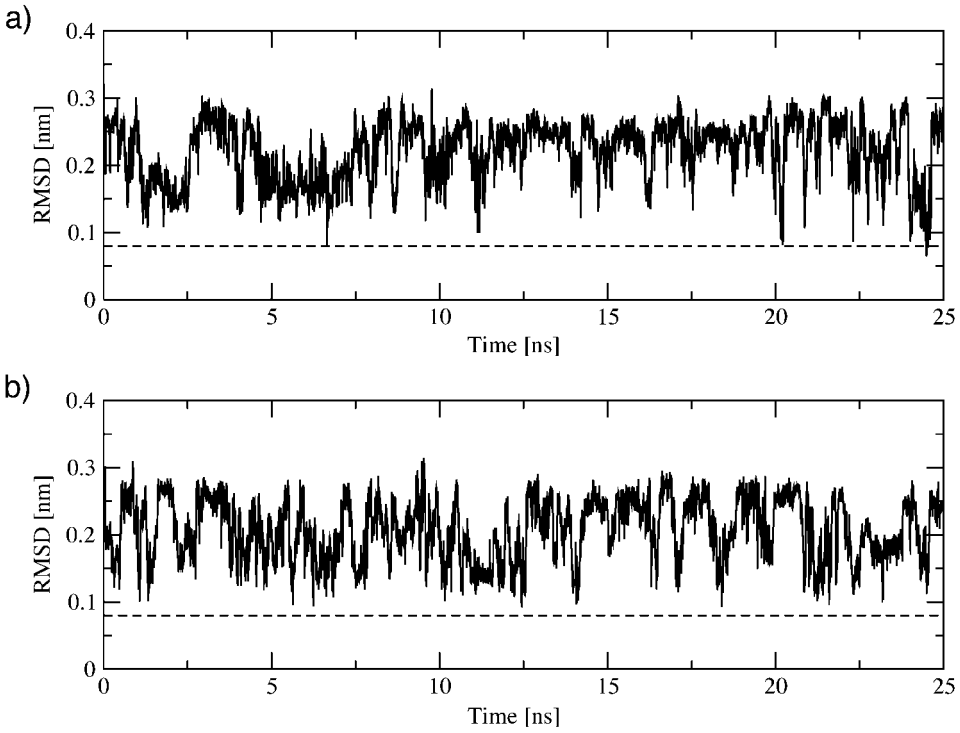

Fig. 9. *Trajectory atom-positional RMSD for molecules* **1** (a) *and* **2** (b) *from the right-handed* 3_1*-helix model* (The configuration used in the calculation of the RMSD is described in the caption of *Fig. 8*)

investigation in $CHCl_3$. It has been shown that the PHB fragment samples its configurational space more or less randomly. Furthermore, it does not significantly populate either of the two helical conformations that have been suggested as possible structures of PHB in solution.

Financial suppoprt from the ERASMUS student exchange program and from the *Swiss National Science Foundation* (project No. 21-50929.97) is gratefully acknowledged (*W. F. v. G.*, *F. A. H.*, *L. D. S.*, and *P. J. G.*). Thanks go to *C. Peter* for help and advice with setting up the first simulations. We thank *C. Griesinger* for helpful discussions. We would like to express our gratitude to *Zeneca Bio Products* (Billingham, GB) for supplying us with PHB and *Novartis Pharma AG* (Basel) for continuing financial support (*D. S.* and *A. M.*). This work was supported by the *MIT*, the *Karl-Winnacker Foundation*, the *Alfred P. Sloan Foundation*, the *NIH* (NCRR Programme), and the *Fonds der Chemischen Industrie* (*H. S.* and *E. D.*).

REFERENCES

[1] D. Seebach, M. G. Fritz, *Biol. Macromolecules* **1999**, *25*, 217.
[2] D. Seebach, A. Brunner, H. M. Bürger, R. N. Reusch, L. L. Bramble, *Helv. Chim. Acta* **1996**, *79*, 507; S. Das, U. D. Lengweiler, D. Seebach, R. N. Reusch, *Proc. Nat. Acad. Sci. U.S.A.* **1997**, *94*, 9075; M. G. Fritz, P. Walde, D. Seebach, *Macromolecules* **1999**, *32*, 574.
[3] R. N. Reusch, *Biochemistry* **2001**, *40*, 2075.
[4] M. Yokouchi, Y. Chatani, H. Tadokoro, K. Teranishi, H. Tani, *Polymer* **1973**, *14*, 267; R. J. Pazur, S. Raymond, P. J. Hocking, R. H. Marchessault, *Polymer* **1998**, *39*, 3065; R. J. Pazur, S. Raymond, P. J. Hocking, R. H. Marchessault, *Macromolecules* **1998**, *31*, 6585.

[5] D. Seebach, A. K. Beck, U. Brändli, D. Müller, M. Przybylski, K. Schneider, *Chimia* **1990**, *44*, 112; D. Seebach, H. M. Bürger, H.-M. Müller, U. D. Lengweiler, A. K. Beck, K. E. Sykes, P. H. Barker, P. J. Barham, *Helv. Chim. Acta* **1994**, *77*, 1099.
[6] D. Seebach, U. Brändli, P. Schnurrenberger, M. Przybylski, *Helv. Chim. Acta* **1988**, *71*, 155; D. Seebach, U. Brändli, H.-M. Müller, M. Dobler, M. Egli, M. Przybylski, K. Schneider, *Helv. Chim. Acta* **1989**, *72*, 1704; H.-M. Müller, M. Dobler, P. Zbinden, D. Seebach, *Chimia* **1991**, *45*, 376; D. Seebach, T. Hoffmann, F. N. M. Kühnle, J. N. Kinkel, M. Schulte, *Helv. Chim. Acta* **1995**, *78*, 1525; A. Brunner, F. M. N. Kühnle, D. Seebach, *Helv. Chim. Acta* **1996**, *79*, 319; D. A. Plattner, Dissertation ETH-Zürich, No. 10283, 1993; F. M. N. Kühnle, Dissertation ETH-Zürich, No. 11782, 1996; D. A. Plattner, A. Brunner, M. Dobler, H.-M. Müller, W. Petter, P. Zbinden, D. Seebach, *Helv. Chim. Acta* **1993**, *76*, 2004; D. Seebach, T. Hoffmann, F. N. M. Kühnle, U. D. Lengweiler, *Helv. Chim. Acta* **1994**, *77*, 2007; B. M. Bachmann, D. Seebach, *Helv. Chim. Acta* **1998**, *81*, 2430.
[7] M. Rueping, A. Dietrich, V. Buschmann, M. G. Fritz, M. Sauer, D. Seebach, *Macromolecules* **2001**, *34*, 7042.
[8] P. Waser, M. Rueping, D. Seebach, E. Duchardt, H. Schwalbe, *Helv. Chim. Acta* **2001**, *84*, 1821.
[9] R. H. Marchessault, K. Okamura, C. J. Su, *Macromolecules* **1970**, *3*, 735.
[10] D. Seebach, M. Overhand, F. N. M. Kühnle, B. Martinoni, L. Oberer, U. Hommel, H. Widmer, *Helv. Chim. Acta* **1996**, *79*, 913; D. Seebach, P. E. Ciceri, M. Overhand, B. Jaun, D. Rigo, L. Oberer, U. Hommel, R. Amstutz, H. Widmer, *Helv. Chim. Acta* **1996**, *79*, 2043; D. Seebach, K. Gademann, J. V. Schreiber, J. L. Matthews, T. Hintermann, B. Jaun, L. Oberer, U. Hommel, H. Widmer, *Helv. Chim. Acta* **1997**, *80*, 2033; D. Seebach, S. Abele, K. Gademann, G. Guichard, T. Hintermann, B. Jaun, J. L. Matthews, J. V. Schreiber, L. Oberer, U. Hommel, H. Widmer, *Helv. Chim. Acta* **1998**, *81*, 932; J. L. Matthews, K. Gademann, B. Jaun, D. Seebach, *J. Chem. Soc. Perkin Trans. 1* **1998**, 3331; D. Seebach, S. Abele, K. Gademann, B. Jaun, *Angew. Chem.* **1999**, *111*, 1700; *Angew. Chem., Int. Ed.* **1999**, *38*, 1595; T. Sifferlen, M. Rueping, K. Gademann, B. Jaun, D. Seebach, *Helv. Chim. Acta* **1999**, *82*, 2067; D. Seebach, A. Jacobi, M. Rueping, K. Gademann, M. Ernst, B. Jaun, *Helv. Chim. Acta* **2000**, *83*, 2115; M. Rueping, B. Jaun, D. Seebach, *Chem. Commun.* **2000**, 2267; X. Daura, K. Gademann, H. Schäfer, B. Jaun, D. Seebach, W. F. van Gunsteren, *J. Am. Chem. Soc.* **2001**, *123*, 2393; P. I. Arvidsson, M. Rueping, D. Seebach, *Chem. Commun.* **2001**, 649.
[11] M. Albert, D. Seebach, E. Duchardt, H. Schwalbe, *Helv. Chim. Acta* **2001**, *85*, 633.
[12] X. Daura, W. F. van Gunsteren, D. Rigo, B. Jaun, D. Seebach, *Chem. Eur. J.* **1997**, *3*, 1410; X. Daura, B. Jaun, D. Seebach, W. F. van Gunsteren, A. E. Mark, *J. Mol. Biol.* **1998**, *280*, 925; X. Daura, K. Gademann, B. Jaun, D. Seebach, W. F. van Gunsteren, A. E. Mark, *Angew. Chem* **1999**, *111*, 249; *Angew. Chem., Int. Ed.* **1999**, *38*, 236; K. Gademann, B. Jaun, D. Seebach, R. Perozzo, L. Scapozza, G. Folkers, *Helv. Chim. Acta* **1999**, *82*, 1; D. Seebach, J. V. Schreiber, S. Abele, X. Daura, W. F. van Gunsteren, *Helv. Chim. Acta* **2000**, *83*, 34.
[13] W. Klyne, V. Prelog, *Experientia* **1960**, *16*, 521.
[14] W. F. van Gunsteren, S. R. Billeter, A. A. Eising, P. H. Hünenberger, P. Krüger, A. E. Mark, W. R. P. Scott, I. G. Tironi, 'Biomolecular Simulation: the GROMOS96 Manual and User Guide', Vdf Hochschulverlag AG an der ETH-Zürich, Zürich, 1996.
[15] I. Tironi, W. F. van Gunsteren, *Mol. Phys.* **1994**, *83*, 381.
[16] W. P. Scott, P. H. Hünenberger, I. Tironi, A. E. Mark, S. R. Billeter, J. Fennen, A. E. Torda, T. Huber, P. Krüger, W. F. van Gunsteren, *J. Phys. Chem. A.* **1999**, *103*, 3596.
[17] H. J. C. Berendsen, J. P. M. Postma, W. F. van Gunsteren, A. DiNola, J. R. Haak, *J. Chem. Phys.* **1984**, *81*, 3684.
[18] I. Tironi, R. Sperb, P. E. Smith, W. F. van Gunsteren, *J. Chem. Phys.* **1995**, *102*, 5451.
[19] J.-P. Ryckaert, G. Ciccotti, H. J. C. Berendsen, *J. Comput. Phys.* **1977**, *23*, 327.
[20] X. Daura, W. F. van Gunsteren, A. E. Mark, *Proteins* **1999**, *34*, 269; D. Seebach, J. V. Schreiber, S. Abele, X. Daura, W. F. van Gunsteren, *Helv. Chim. Acta* **2000**, *83*, 34; X. Daura, K. Gademann, H. Schäfer, B. Jaun, D. Seebach, W. F. van Gunsteren, *J. Am. Chem. Soc.* **2001**, *123*, 2393.
[21] M. J. Karplus, *Chem. Phys.* **1959**, *30*, 11.
[22] C. A. G. Haasnoot, F. A. A. M. de Leeuw, C. Altona, *Tetrahedron* **1979**, *36*, 2783.
[23] V. F. Bystrov, *Prog. Nucl. Magn. Reson. Spectrosc.* **1976**, *10*, 41.
[24] M. L. Huggins, *J. Am. Chem. Soc.* **1953**, 75, 4123.
[25] D. Yang, F.-F. Ng, Z.-J. Li, Y.-D. Wu, K. W. Chan, D.-P. Wang, *J. Am. Chem. Soc.* **1999**, *121*, 589.
[26] C. Peter, X. Daura, W. F. van Gunsteren, *J. Am. Chem. Soc.* **2000**, *122*, 7461.

Received September 7, 2000